

## Preparation of Hydrochar from *Salacca zalacca* Peels by Hydrothermal Carbonization: Study of Adsorption on Congo Red Dyes and Regeneration Ability

Mauizatul Hasanah<sup>1,3</sup>, Alfian Wijaya<sup>2</sup>, Fitri Suryani Arsyad<sup>3</sup>, Risfidian Mohadi<sup>3\*</sup>, Aldes Lesbani<sup>2,3</sup>

<sup>1</sup>Department of Pharmacy, School of Pharmacy Bhakti Pertiwi, Palembang, 30128, Indonesia

<sup>2</sup>Research Centre of Inorganic Materials and Coordination Complexes, Faculty of Mathematics and Natural Sciences, Sriwijaya University, Palembang, 30139, Indonesia

<sup>3</sup>Doctoral Program, Faculty of Mathematics and Natural Sciences, Sriwijaya University, Palembang, 30139, Indonesia

\*Corresponding author: risfidian.mohadi@unsri.ac.id

### Abstract

Hydrochar of *Salacca zalacca* peels (HC-SP) is prepared by hydrothermal carbonization treatment of *Salacca zalacca* peels (SP) obtained from local fruits at Palembang, South Sumatera, Indonesia, with the resulting yield weight reaching 90%. Materials are characterized using the XRD diffraction, FTIR spectrum, and SEM-EDX. The XRD pattern shows the characteristics of the formation of amorphous compounds. The FTIR spectrum confirms the presence of functional groups O-H, C-H, C=C, and C-O. Data of SEM-EDX show that materials have heterogeneous morphologies, form aggregates, and in HC-SP materials there is an increase in carbon content from the initial material. The capacity of SP in the congo red (CR) adsorption process is 33.003 mg/g and increases to 133.333 mg/g in HC-SP. The maximum dye adsorbed was achieved at pH 4. The adsorption kinetics followed PSO with the equilibrium adsorption occurring at 90 minutes, and the adsorption isotherm followed the Langmuir isotherm with the value of  $R^2$  closer to the value of 1. A positive  $\Delta H$  value indicated that the adsorption is an endothermic process. In contrast, an  $\Delta S$  value suggested that the degree of irregularity in the adsorption process is small in large concentrations. Based on data regeneration ability, materials of SP and HC-SP can be used in the three cycles regeneration process of the CR adsorption process. The adsorption process of CR occurs physically and chemically based on enthalpy values and FT-IR data after being adsorbed with CR.

### Keywords

Hydrochar, *Salacca zalacca* Peels, Adsorption, Congo Red, Regeneration

Received: 20 March 2022, Accepted: 14 July 2022

<https://doi.org/10.26554/sti.2022.7.3.372-378>

## 1. INTRODUCTION

Hydrothermal carbonization (HTC) is a thermochemical process to convert biomass into rich-carbon materials, often referred to as hydrochar. This process has the advantage of using milder temperatures (180-250°C) and water that acts as a solvent and catalyst. The favorable reaction conditions make this process more economically feasible compared to other chemical processes (Yu et al., 2022; Camilo et al., 2021; Liu et al., 2022). Carbon-based materials such as hydrochar have high chemical stability, porous structure, physical and chemical properties, and surface area (Zulfajri et al., 2021). Recently, some literature reported the successful preparation of hydrochar from natural resources such as rice husk (Phan et al., 2022), avocado seed (Dhaouadi et al., 2021), sewage sludge, and coconut shell (Tu et al., 2021), coffee waste (Santana et al., 2022), banana peels (Yusuf et al., 2020), pomelo peels (Wei et al., 2022) and orange peels (Espro et al., 2021).

*Salacca zalacca* (snake fruits) peels one of the biomass pro-

duced from agricultural waste easily obtained in Indonesia (Fatimah et al., 2022). Research conducted by Fatimah et al., 2021; Arie et al., 2018 shows the ability of *Salacca zalacca* peels in dye removal, to improve its adsorption ability, treatment is carried out through hydrothermal carbonization in this study. Hydrochar is widely used as an adsorbent and is primarily utilized as an effective and reliable treatment for removing dye pollutants (Haris et al., 2022; Zulfajri et al., 2021). Dye pollutants are produced from factories that produce textile clothing, medicines, and food products. Synthetic dyes are difficult to remove due to the complex aromatic structure. One of the widely used dyes is congo red (CR). Dye pollutants are highly toxic, carcinogenic, difficult to biodegrade, and have high solubility in water. Water contaminated with dyes will adversely affect organisms in the water and is very dangerous if exposed to the human body (Kenawy et al., 2022). Therefore, it is necessary to have an effective method for the removal of dye pollutants. Many ways to remove the dye pollutants like coagulation-flocculation (Ihaddaden et al., 2022), pho-



**Figure 1.** Schematic Representation of Hydrochar Preparation

tocatalysis (Mahmoodi et al., 2022), oxidation-precipitation (Anushree and Philip, 2019), and adsorption (Tran et al., 2020; Wijaya et al., 2021; Palapa et al., 2021). Comparing some of these methods, adsorption is one of the economic processes in wastewater treatment and is considered an easy, efficient technique for its operation, high efficiency, and low cost (Karthi et al., 2022).

According to research by Haris et al. (2022), hydrochar made from olive waste showed high effectiveness in removing methylene blue and congo red dyes from water. Hydrochar from straw mushrooms conducted by Zulfajri et al. (2021) and applied to removal of dyes i.e. crystal violet and methylene blue, showed excellent removal efficiencies of more than 90%. In this research, the preparation of hydrochar was retrieved from *Salacca zalacca* peels which is residual waste, and then materials were analyzed using XRD, FT-IR, and SEM-EDX. It will be applied as adsorbents to remove congo red dyes and study the effect of pH, times, adsorption isotherm, adsorption thermodynamics, and regeneration ability.

## 2. EXPERIMENTAL SECTION

### 2.1 Chemicals and Instrumentation

The materials used in this study such as *Salacca zalacca* peels were obtained from the local fruits at Palembang, South Sumatera, Indonesia. Chemicals include orthophosphoric acid, distilled water, HCl, NaOH, NaCl, and anionic dyes (congo red (CR)). The material was characterized using an X-Ray Rigaku Miniflex-600 diffractometer, Shimadzu Prestige-21 FTIR Spectrophotometer, Scanning Electron Microscope Energy Dispersive Spectrometer (SEM-EDS) Quanta 650, and absorbance measurement of solution using UV-Visible Biobase Spectrophotometer UV BK-1800PC.

### 2.2 Preparation of Hydrochar from *Salacca zalacca* Peels

*Salacca zalacca* peels are dried in the sun and then crushed and filtered. As much as 2 g of *Salacca zalacca* peels powder, and 50 mL of orthophosphoric acid were added to the hydrothermal stainless steel autoclave, then heated at a temperature of 150°C for 6 hours. The mixture was filtered and heated at 110°C

for 6 hours. The obtained material was characterized using XRD, FTIR, and SEM-EDX. A schematic representation of hydrochar preparation showed in Figure 1.

### 2.3 Study of Adsorption

The study of adsorption was carried out with 3 treatments: the effect of pH, contact time adsorption, and concentration temperature adsorption. The effect of pH can be studied by pH pzc treatment and pH adsorption. pH pzc can be studied by varying the pH of the NaCl solution (2-11), then adding 0.02 g of material to the solution and stirring for 24 hours. The pH effect of adsorption can be studied by varying the pH of CR (4-11), and the effect of contact time adsorption on anionic dyes can be studied by varying the contact time (0, 10, 20, 30, 40, 50, 60, 70, 80, 90, 100, 120, 150, and 180 minutes). As much as 0.02 g adsorbents were added to an Erlenmeyer containing 20 mL of dye solution with a concentration of 50 mg/L, and the mixture was stirred. The effect of concentration and temperature adsorption was studied by varying the concentration (60, 70, 80, 90, and 100 mg/L) and temperature (30, 40, 50, 60, and 70°C). As much as 0.02 g adsorbents were added to an Erlenmeyer containing 20 mL of dye solution and stirred for 60 minutes. The filtrate was measured using a UV-Vis spectrophotometer.

### 2.4 Study of Regeneration Ability

Regeneration of adsorbent is carried out by adsorption and desorption processes first. Dyes 50 mg/L were added to 0.1 g of adsorbent. The mixture was stirred for 2 hours, and the absorbance of the filtrate was measured using a UV-Visible spectrophotometer. Adsorbents that have been used in the adsorption process are carried out the desorption process with ultrasonic systems that use water. Dried adsorbents are used in the adsorption process for the next cycle.

## 3. RESULTS AND DISCUSSION

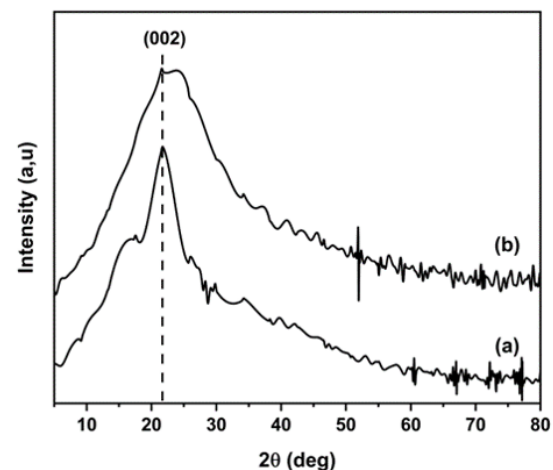


**Figure 2.** Diffraction Patterns of SP (a) and HC-SP (b)

Preparation of HC-SP by hydrothermal carbonization treatment (Figure 1) results in weight yields up to 90%. X-ray diffractogram pattern of the *Salacca zalacca* peels (SP) and hydrochar of *Salacca zalacca* peels (HC-SP) are shown in Figure 2. A broad peak at a diffraction angle of around 20° with field diffraction (002) indicates that the material has low crystallinity and shows the characteristics of the formation of amorphous compounds.

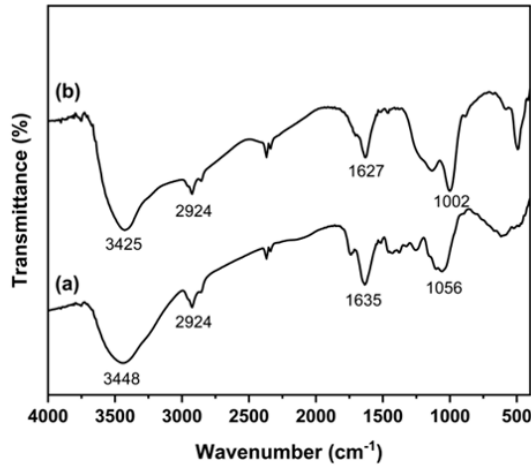


Figure 3. FT-IR Spectrum of SP (a) and HC-SP (b)

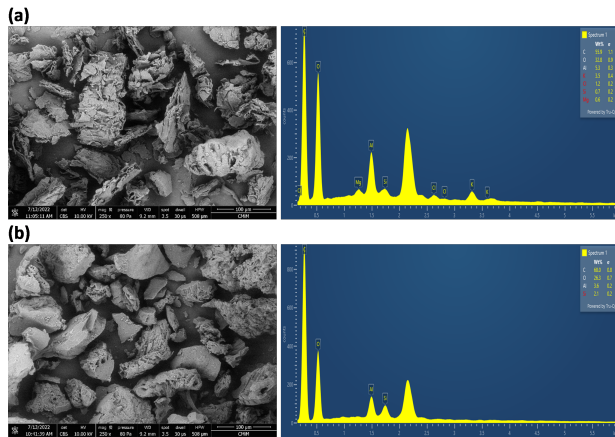


Figure 4. SEM-EDX of SP (a) and HC-SP (b)

The spectrum FT-IR of SP and HC-SP are shown in Figure 3. The FT-IR spectrum of SP in Figure 3(a) shows that the peak at wavenumber 3448, 2924, 1635, and 1056  $\text{cm}^{-1}$  corresponds to the presence of O-H, C-H, C=C, and C-O functional groups, respectively. The functional group of SP in this research is similar to the results of the study reported by Fatimah et al. (2021). The FT-IR spectrum of HC-SP in Figure 3(b) experienced a not-so-significant shift in the wavenumber from the starting material due to hydrothermal carbonization treatment. Data of SEM-EDX is shown in Figure 4 with a magnification of 250 times. SEM-EDX data shows that SP and

HC-SP materials have heterogeneous morphologies and form aggregates, and the morphology of HC-SP looks more refined compared to SP. In HC-SP materials, there is an increase in carbon content from the initial material due to hydrothermal carbonization treatment. In SP material, the percent of the carbon content weight is 55.9% increasing to 68% in HC-SP material. This proves the success of the hydrothermal carbonization process that has been carried out in this research.

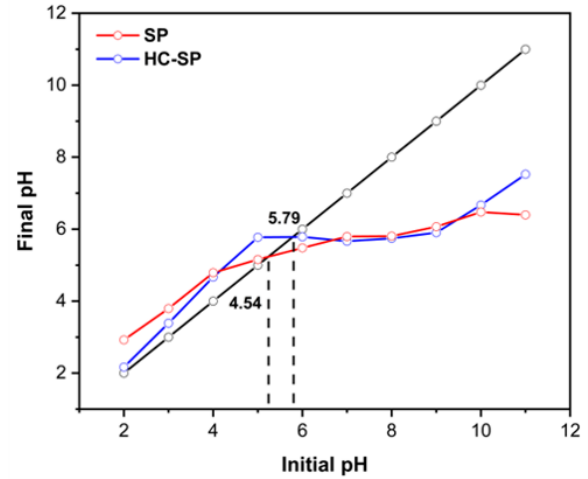


Figure 5. pH pzc of Materials

The results of the pH pzc treatment can be seen in Figure 5. Based on the data of pH pzc, it can be seen that the pH pzc of SP and HC-SP materials are 4.54 and 5.79, respectively. In adsorption treatment, if the material is contacted with a solution whose pH is below pH pzc, then the material's surface is positively charged and in reverse. Based on this statement, the adsorption process of anionic dyes such as CR is more suitable to be carried out under pH pzc.

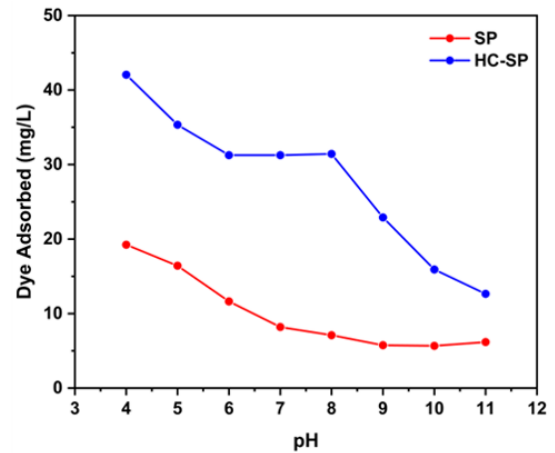
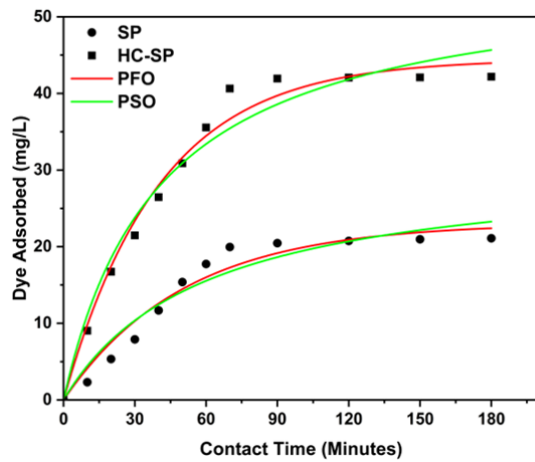


Figure 6. Effect of pH on Adsorption Process

Materials of SP and HC-SP were applied as adsorbents to the removal of CR and studying the effect of pH, times, adsorp-

**Table 1.** Adsorption Kinetic Parameters

Adsorbents	Initial Concentration (mg/L)	$Q_{e_{exp}}$ (mg/g)	$Q_{e_{calc}}$ (mg/g)	PFO		PSO		
				$R^2$	$k_1$	$Q_{e_{calc}}$ (mg/g)	$R^2$	$k_2$
SP	50.059	21.092	29.282	0.967	0.038	23.641	0.991	0.002
HC-SP	50.059	42.185	66.374	0.936	0.049	54.348	0.972	0.0005



**Figure 7.** Adsorption Kinetic Models

tion isotherm, adsorption thermodynamics, and regeneration ability. Based on the data on the development of pH in the CR adsorption process in Figure 6, it can be seen that the highest adsorption concentration is at pH 4. In contrast, at an increase in pH from 4-9, there is a continuous decrease in the dye adsorbed, similar to the reported by Brahma and Saikia (2022). The results of this adsorption pH are in accordance with the pH pzc statement above, where the CR adsorption process is more suitable to be carried out below the pH pzc. Adsorption kinetic models and kinetic parameters are shown in Figure 7 and Table 1, respectively. Based on the results of adsorption kinetic models shown in Figure 7, the equilibrium adsorption of CR occurred at 90 minutes, with an insignificant increase in adsorption concentration at a contact time of more than 90 minutes, and based on data, Table 1 shows that the adsorption kinetics followed PSO, with the value of the linear regression coefficient ( $R^2$ ) which is close to the value 1.

Adsorption isotherm models and isotherm adsorption are shown in Figure 8 and Table 2, respectively. Based on the adsorption isotherm of SP and HC-SP in Figure 8 indicates that increasing temperature causes the increase in adsorption concentration, and adsorption concentrations in HC-SP are higher than with SP. Table 2 shows the large adsorption capacity that occurred at an adsorption temperature of 70°C and occurred an increase of adsorption capacity in HC-SP during the CR adsorption process. The adsorption capacity of SP is 33.003 mg/g to be 133.333 mg/g in HC-SP. This proves

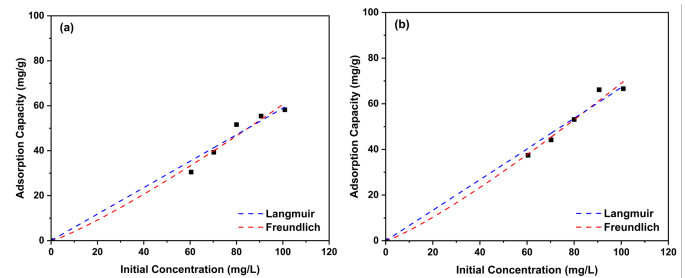


**Figure 8.** Adsorption Isotherm Models of SP (a) and HC-SP (b)

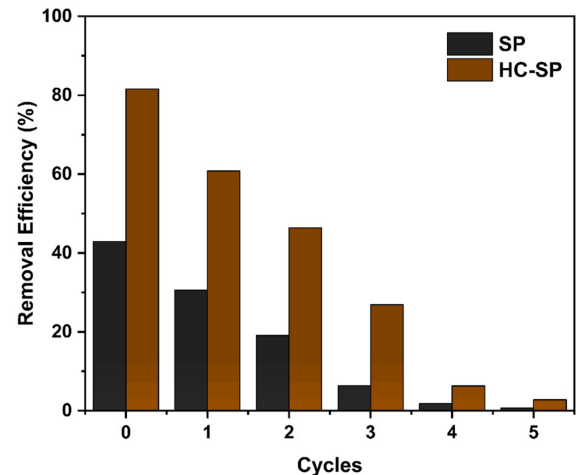


**Figure 9.** Regeneration Ability of SP and HC-SP

that hydrothermal carbonization treatment will improve the performance of the material. Based on Figure 8 and Table 2, it can be seen that the Langmuir model is better than the Freundlich model for the adsorption process in this study, with the value of  $R^2$  closer to the value of 1. Adsorption thermodynamic parameters are shown in Table 3. The enthalpy ( $\Delta H$ ) value offers the range of 6.693 to 18.097 kJ/mol, indicating the physical adsorption process. Generally, an enthalpy value of less than 21 kJ/mol indicated adsorption physics (Nimibofa et al., 2017) A positive  $\Delta H$  value indicated that the adsorption is an endothermic process, while an  $\Delta S$  value suggested that the degree of irregularity in the adsorption process is small in large concentrations.

The regeneration ability of SP and HC SP is shown in

**Table 2.** Adsorption Isotherm Parameters

Adsorbents	Adsorption Isotherm	Adsorption Constant	T (K)				
			30°C	40°C	50°C	60°C	70°C
SP	Langmuir	Q <sub>max</sub>	10.604	15.456	18.762	28.986	33.003
		k <sub>L</sub>	0.016	0.016	0.017	0.016	0.016
		R <sup>2</sup>	0.998	0.999	0.999	0.999	0.999
	Freundlich	n	0.312	0.411	0.510	0.685	0.774
		k <sub>F</sub>	12.210	11.112	11.508	5.055	2.497
		R <sup>2</sup>	0.999	0.998	0.995	0.999	0.997
HC-SP	Langmuir	Q <sub>max</sub>	26.810	27.397	78.125	101.010	133.333
		k <sub>L</sub>	0.013	0.016	0.011	0.012	0.013
		R <sup>2</sup>	0.995	0.951	0.999	0.999	0.999
	Freundlich	n	0.470	0.442	0.531	0.503	0.229
		k <sub>F</sub>	10.541	10.859	15.581	13.868	10.447
		R <sup>2</sup>	0.805	0.976	0.934	0.869	0.989

**Table 3.** Adsorption Thermodynamic Parameters

Adsorbents	Concentration (mg/L)	T (K)	Q <sub>e</sub> (mg/g)	ΔH (kJ/mol)	ΔS (J/mol. K)	ΔG (kJ/mol)
SP	100.874	303	50.731	6.693	0.022	-0.015
		313	52.454			-0.236
		323	54.681			-0.457
		333	56.866			-0.679
		343	58.210			-0.900
HC-SP	100.874	303	51.866	18.097	0.060	-0.040
		313	55.689			-0.639
		323	61.109			-1.237
		333	66.613			-1.836
		343	71.277			-2.435

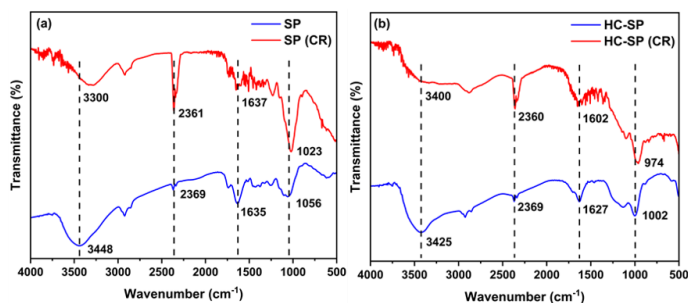


**Figure 10.** FT-IR Spectrum of SP (a) and HC-SP (b) after CR Adsorption

Figure 9. Based on Figure 9, it can be seen that the adsorption ability decreases as the regeneration cycle increases and there is a significant decrease in adsorption ability in the fourth and fifth cycles. Materials of SP and HC-SP can be used in the

three cycles regeneration process of CR adsorption process. FT-IR spectrum of SP and HC-SP after CR adsorption is shown in Figure 10. Based on Figure 10, it can be seen that in SP and HC-SP materials after being adsorbed CR, there is a shift in the wavenumber and a change in intensity from the initial material. It is caused by the chemical interaction that occurs in the adsorption process between the material and CR, it indicates that the adsorption process that occurs is also chemically. The shift in the wavenumber and the change in intensity in the area of about 3400 and 1000 cm<sup>-1</sup> indicate the presence of hydrogen bonds (H-O-H) that occur between the SP and HC-SP materials with CR, while the shift in the wave numbers and changes in the intensity in the wave number areas of about 2300 and 1600 cm<sup>-1</sup> indicate an increase in the C-H and C=C bonds due to the binding of CR to the material.

A comparison of the adsorption capacity of CR by several adsorbents from natural resources or waste can be seen in Table 4. Based on the data in Table 4, it can be seen that HC-SP

**Table 4.** Adsorption Capacity of CR by several Adsorbents

Adsorbents	Adsorption Capacity (mg/g)	References
<i>Aspergillus carbonarius</i> M333	99.01	(Dhaouadi et al., 2021)
<i>Penicillium glabrum</i> Pg1	101.01	(Dhaouadi et al., 2021)
Chemically Modified Egg Shell Membrane	117.65	(Parvin et al., 2019)
Tunics of the Corm of the Saffron	6.2	(Dbik et al., 2020)
Cabbage Waste Powder	2.313	(Wekoye et al., 2020)
Red Dragon Fruit Peel	71.74	(Lima et al., 2021)
Iron Oxide from Steel Waste Recycling Produced with Bottle Cap	104.17	(Borth et al., 2021)
Vermicompost	23.25	(Ribeiro et al., 2021)
HC-SP	133.333	This Research

has a higher adsorption capacity in the CR adsorption process compared to other adsorbents, thus it can be said that HC-SP is a potential material that can be used in removing CR.

#### 4. CONCLUSION

The success of the preparation of HC-SP by hydrothermal carbonization was proven by the characterization of XRD, FT-IR, and SEM-EDX. In this study, the material was applied as an adsorbent for CR by studying the study of adsorption and regeneration ability. The maximum dye adsorbed was achieved at pH 4. The adsorption kinetics followed PSO with the equilibrium adsorption occurring at 90 minutes and the adsorption isotherm followed the Langmuir isotherm with the value of  $R^2$  closer to the value of 1. The adsorption capacity of SP in the CR adsorption process is 33.003 mg/g and increases to 133.333 mg/g in HC-SP. Adsorption in this study includes an endothermic process and occurs spontaneously. Based on data regeneration ability, materials of SP and HC-SP can be used in the three cycles regeneration process of the CR adsorption process. The adsorption process of CR occurs physically and chemically based on enthalpy values and FT-IR data after being adsorbed with CR.

#### 5. ACKNOWLEDGMENT

The authors thank to Research Center of Inorganic Materials and Coordination Complexes FMIPA Universitas Sriwijaya for support and instrumental analysis.

#### REFERENCES

- Anushree, C. and J. Philip (2019). Efficient Removal of Methylene Blue Dye Using Cellulose Capped Fe<sub>3</sub>O<sub>4</sub> Nanofluids Prepared Using Oxidation Precipitation Method. *Colloids and Surfaces A: Physicochemical and Engineering Aspects*, **567**; 193–204
- Arie, A. A., H. Kristianto, and F. Apecsiana (2018). Adsorption of Cu (II) from Aqueous Solution by Salacca Peel Based Activated Carbons. *Journal of Chemistry and Applied Chemical Engineering*, **2**(1); 1–9
- Borth, K. W., C. W. Galdino, V. de Carvalho Teixeira, and F. J. Anaissi (2021). Iron Oxide Nanoparticles Obtained From Steel Waste Recycling as a Green Alternative for Congo Red Dye Fast Adsorption. *Applied Surface Science*, **546**; 149126
- Brahma, D. and H. Saikia (2022). Synthesis of ZrO<sub>2</sub>/MgAl-LDH Composites and Evaluation of its Isotherm, Kinetics and Thermodynamic Properties in the Adsorption of Congo Red Dye. *Chemical Thermodynamics and Thermal Analysis*; 100067
- Camilo, F. C., T. P. de Araujo, H. B. Quesada, A. A. Moura, M. P. Moises, R. Bergamasco, S. H. Faria, and M. A. S. D. de Barros (2021). Synthesis of Hydrochars Derived from Industrial Laundry Sludge and its Application in the Removal of Cationic Dye. *Journal of Water Process Engineering*, **40**; 101999
- Dbik, A., S. Bentahar, M. El Khomri, N. El Messaoudi, and A. Lacherai (2020). Adsorption of Congo Red Dye from Aqueous Solutions Using Tunics of the Corm of the Saffron. *Materials Today: Proceedings*, **22**; 134–139
- Dhaouadi, F., L. Sellaoui, L. E. Hernández-Hernández, A. Bonilla-Petriciolet, D. I. Mendoza-Castillo, H. E. Reynel-Ávila, H. A. González-Ponce, S. Taamalli, F. Louis, and A. B. Lamine (2021). Preparation of an Avocado Seed Hydrochar and its Application as Heavy Metal Adsorbent: Properties and Advanced Statistical Physics Modeling. *Chemical Engineering Journal*, **419**; 129472
- Espro, C., A. Satira, F. Mauriello, Z. Anajafi, K. Moulae, D. Iannazzo, and G. Neri (2021). Orange Peels Derived Hydrochar for Chemical Sensing Applications. *Sensors and Actuators B: Chemical*, **341**; 130016
- Fatimah, I., G. Purwiandono, I. Sahroni, A. Wijayana, M. Faraswati, A. D. Putri, W.-C. Oh, and R.-a. Doong (2022). Magnetically Separable Photocatalyst of Magnetic Biochar from Snake Fruit Peel for Rhodamine B Photooxidation. *Environmental Nanotechnology, Monitoring & Management*, **17**; 100669
- Fatimah, I., I. Sahroni, M. S. E. Dahlyani, A. M. N. Oktaviyani, and R. Nurillahi (2021). Surfactant Modified Salacca zalacca Skin as Adsorbent for Removal of Methylene Blue

- and Batik's Wastewater. *Materials Today: Proceedings*, **44**; 3211–3216
- Haris, M., M. W. Khan, J. Paz-Ferreiro, N. Mahmood, and N. Eshtiaghi (2022). Synthesis of Functional Hydrochar from Olive Waste for Simultaneous Removal of Azo and Non Azo Dyes from Water. *Chemical Engineering Journal Advances*, **9**; 100233
- Ihaddaden, S., D. Aberkane, A. Boukerroui, and D. Robert (2022). Removal of Methylene Blue (Basic Dye) by Coagulation Flocculation with Biomaterials (Bentonite and Opuntia Ficus Indica). *Journal of Water Process Engineering*, **49**; 102952
- Karthi, S., R. Sangeetha, K. Arumugam, T. Karthika, and S. Vimala (2022). Removal of Methylene Blue Dye Using Shrimp Shell Chitin from Industrial Effluents. *Materials Today: Proceedings*
- Kenawy, E.-R., H. Tenhu, S. A. Khattab, A. A. Eldeeb, and M. M. Azaam (2022). Highly Efficient Adsorbent Material for Removal of Methylene Blue Dye Based on Functionalized Polyacrylonitrile. *European Polymer Journal*, **169**; 111138
- Lima, L. B., N. Priyanthab, S. A. A. Latipa, and Y. Lua (2021). Sequestration of Toxic Congo Red Dye Through the Utilization of Red Dragon Fruit Peel: Linear Versus Nonlinear Regression Analyses of Isotherm and Kinetics. *Desalination And Water Treatment*, **218**; 409–422
- Liu, X., J. Lu, M. Fu, H. Zheng, and Q. Chen (2022). Activated Carbon Induced Hydrothermal Carbonization for the Treatment of Cotton Pulp Black Liquor. *Journal of Water Process Engineering*, **47**; 102733
- Mahmoodi, M., E. Rafiee, and S. Eavani (2022). Photocatalytic Removal of Toxic Dyes, Liquorice and Tetracycline Wastewaters by a Mesoporous Photocatalyst Under Irradiation of Different Lamps and Sunlight. *Journal of Environmental Management*, **313**; 115023
- Nimibofa, A., E. Augustus, and D. Wankasi (2017). Comparative Sorption Studies of Dyes and Metal Ions by Ni/Al Layered Double Hydroxide. *Internasional Journal of Material and Chemistry*, **7**(3); 25–35
- Palapa, N. R., T. Taher, A. Wijaya, and A. Lesbani (2021). Modification of Cu/Cr Layered Double Hydroxide by Keggin Type Polyoxometalate as Adsorbent of Malachite Green from Aqueous Solution. *Science and Technology Indonesia*, **6**(3); 209–217
- Parvin, S., B. K. Biswas, M. A. Rahman, M. H. Rahman, M. S. Anik, and M. R. Uddin (2019). Study on Adsorption of Congo Red Onto Chemically Modified Egg Shell Membrane. *Chemosphere*, **236**; 124326
- Phan, K. A., D. Phihusut, and N. Tuntiwiwattanapun (2022). Preparation of Rice Husk Hydrochar as an Atrazine Adsorbent: Optimization, Characterization, and Adsorption Mechanisms. *Journal of Environmental Chemical Engineering*, **10**(3); 107575
- Ribeiro, J. N., A. V. F. Ribeiro, A. R. da Silva, M. de Godoi Pereira, J. P. de Oliveira, A. T. Tomaz, and B. Vitoria (2021). Vermicompost for Indigo Blue and Congo Red Removal. *Journal of Water Resource and Protection*, **13**(6); 419–434
- Santana, M. S., R. P. Alves, L. S. Santana, M. A. Gonçalves, and M. C. Guerreiro (2022). Structural, Inorganic, and Adsorptive Properties of Hydrochars Obtained by Hydrothermal Carbonization of Coffee Waste. *Journal of Environmental Management*, **302**; 114021
- Tran, T. H., A. H. Le, T. H. Pham, D. T. Nguyen, S. W. Chang, W. J. Chung, and D. D. Nguyen (2020). Adsorption Isotherms and Kinetic Modeling of Methylene Blue Dye Onto a Carbonaceous Hydrochar Adsorbent Derived from Coffee Husk Waste. *Science of the Total Environment*, **725**; 138325
- Tu, W., Y. Liu, Z. Xie, M. Chen, L. Ma, G. Du, and M. Zhu (2021). A Novel Activation Hydrochar via Hydrothermal Carbonization and KOH Activation of Sewage Sludge and Coconut Shell for Biomass Wastes: Preparation, Characterization and Adsorption Properties. *Journal of Colloid and Interface Science*, **593**; 390–407
- Wei, Y., S. Fakudze, Y. Zhang, R. Ma, Q. Shang, J. Chen, C. Liu, and Q. Chu (2022). Co Hydrothermal Carbonization of Pomelo Peel and PVC for Production of Hydrochar Pellets with Enhanced Fuel Properties and Dechlorination. *Energy*, **239**; 122350
- Wekoye, J. N., W. C. Wanyonyi, P. T. Wangila, and M. K. Tonui (2020). Kinetic and Equilibrium Studies of Congo Red Dye Adsorption on Cabbage Waste Powder. *Environmental Chemistry and Ecotoxicology*, **2**; 24–31
- Wijaya, A., P. M. S. B. N. Siregar, A. Priambodo, N. R. Palapa, T. Taher, and A. Lesbani (2021). Innovative Modified of Cu-Al/C (C= Biochar, Graphite) Composites for Removal of Procion Red from Aqueous Solution. *Science and Technology Indonesia*, **6**(4); 228–234
- Yu, Y., Y. Guo, G. Wang, Y. A. El-Kassaby, and S. Sokhansanj (2022). Hydrothermal Carbonization of Waste Ginkgo Leaf Residues for Solid Biofuel Production: Hydrochar Characterization and Its Pelletization. *Fuel*, **324**; 124341
- Yusuf, I., F. Flagiello, N. I. Ward, H. Arellano-García, C. Avignone-Rossa, and M. Felipe-Sotelo (2020). Valorisation of Banana Peels by Hydrothermal Carbonisation: Potential Use of the Hydrochar and Liquid by Product for Water Purification and Energy Conversion. *Bioresource Technology Reports*, **12**; 100582
- Zulfajri, M., Y.-T. Kao, and G. G. Huang (2021). Retrieve of Residual Waste of Carbon Dots Derived from Straw Mushroom as a Hydrochar for the Removal of Organic Dyes from Aqueous Solutions. *Sustainable Chemistry and Pharmacy*, **22**; 100469